

## A Compact Miniaturized Flow System Based on Low-Temperature Co-fired Ceramic Technology Coupled to LED Mini-photometer for Determination of Dipyrone in Pharmaceutical Formulations

Willian T. Suarez,<sup>\*a</sup> Osmundo D. Pessoa-Neto,<sup>b</sup> Vagner B. dos Santos,<sup>b</sup> Ana Rita de A. Nogueira,<sup>c</sup> Ronaldo C. Faria,<sup>b</sup> Orlando Fatibello-Filho<sup>b</sup> and Julián A. Chamarro<sup>d</sup>

<sup>a</sup>Departamento de Química, Centro de Ciências Exatas e Tecnológicas, Universidade Federal de Viçosa, 36570-000 Viçosa-MG, Brazil

<sup>b</sup>Departamento de Química, Centro de Ciências Exatas e de Tecnologia, Universidade Federal de São Carlos, 13560-905 São Carlos-SP, Brazil

<sup>c</sup>Embrapa Pecuária Sudeste, 13560-970 São Carlos-SP, Brazil

<sup>d</sup>Sensors and Biosensors Group, Department of Chemistry, Facultat de Ciències, Edifici Cn, Universitat Autònoma de Barcelona, Bellaterra, 08193, Spain

Neste trabalho, a aplicação de um microsistema analítico construído com tecnologia LTCC (cerâmica cossinterizada a baixa temperatura) com incorporação monolítica de uma cela óptica de fluxo para determinação de dipirone em formulações farmacêuticas é descrita. O sistema de detecção baseou-se na formação de um cromóforo azul entre a dipirone e Fe(III) monitorado fotometricamente em 630 nm usando um minifotômetro de LED *lab-made* construído com um diodo emissor de luz como fonte de radiação e um fotodiodo de Si como detector. O minifotômetro elaborado apresentou um bom desempenho com respeito à elevada relação sinal ruído, baixo ruído e sensibilidade satisfatória. A curva analítica foi linear na região de concentração de dipirone de  $1,0 \times 10^{-4}$  a  $3,5 \times 10^{-3}$  mol L<sup>-1</sup> tendo sido obtido um limite de detecção de  $4,5 \times 10^{-5}$  mol L<sup>-1</sup> e um tempo total de análise de 20 s equivalente à uma frequência analítica de 195 h<sup>-1</sup> com pouca geração de resíduos por análise (480 µL).

In this work, an analytical microsystem based on LTCC (low-temperature co-fired ceramic) technology with monolithic incorporation of an optical flow cell for determination of dipyrone in pharmaceuticals is described. The detection system is based on the formation of a blue chromophore between dipyrone and Fe(III) photometrically monitored at 630 nm using a lab-made LED mini-photometer constructed with a light emitting diode as a radiation source and a Si photodiode as a detector. The lab-made mini-photometer elaborated presented a good performance in regard to high signal/noise ratio, low drift and good sensitivity. The analytical curve was linear in the dipyrone concentration range from  $1.0 \times 10^{-4}$  to  $3.5 \times 10^{-3}$  mol L<sup>-1</sup>, limit of detection of  $4.5 \times 10^{-5}$  mol L<sup>-1</sup> and total time of analyses of 20 s yielding an analytical frequency of 195 h<sup>-1</sup> with a low waste generation *per* analysis (480 µL).

**Keywords:** low-temperature co-fired ceramic, analytical microsystem, dipyrone, flow injection analysis, LED photometer

### Introduction

The low-temperature co-fired ceramic (LTCC) or green tape is a new material that has been used as an alternative technology for the fabrication of micro total analysis systems (µ-TAS)<sup>1-3</sup> due to the combination of some of

its main features: rapid prototyping that permits quick modification, the possibility of fabricating 3D structures using multiple layers of green tape without showing deficiencies, there is no need for sealing elements (e.g., epoxies), low fabrication cost (e.g., no need for clean rooms), and it is environmentally friendly.<sup>4,7</sup>

However, due to the small optical path of the analytical microsystems, the absorption of electromagnetic

\*e-mail: williants@ufv.br

radiation by the analyte is limited even for samples in which its concentration is relatively high.<sup>8</sup> Therefore, absorption measurements employing instruments based on photometric detectors based on light emitting diode (LED) and photodiode need to be efficiently amplified.

According to the literature, an operational amplifier (OP) is a device widely employed for this purpose due to its low cost, small size, high signal/noise ratio, good stability and low drift, which permit adequate amplification. Additionally, some lab-made photometers based on LEDs and photodiode present similar performance to that found in commercial photometers and spectrophotometers, and may present greater portability and robustness than these commercial instruments, especially when they are applied to flow injection analysis.<sup>9-11</sup>

Currently, the search for high quality manufactured products, particularly pharmaceuticals, has stimulated the development of rapid analytical methods that require less consumption of reagents, clean procedures and a greater amount of information with regard to chemical composition. In addition to these requirements, the new analytical methods must ensure reliability, precision and accurate results, with a low analysis cost.<sup>12</sup> Flow injection analysis (FIA) has been mainly used for analyte determination in pharmaceutical formulations and quality control applications. This technique is characterized by its simplicity and speed, the inexpensive equipment needed, and the accuracy of its results.<sup>12-14</sup> Compared to batch methods, it offers an increase in sample throughput, high versatility and low consumption of reagents.

The coupling of a microchip to a flow injection system is very interesting because it unites the advantages of both and can substantially improve the analytical characteristics of the system. There are several advantages for FIA miniaturization, such as reproducibility, low analysis time, allowing up to 300 determinations  $\text{h}^{-1}$ , and the reducing of reagent consumption and waste generation.<sup>5</sup> Thus, different types of FIA microsystems have been proposed in the literature for the determination of several analytes.<sup>15-18</sup>

Dipyrone (noramidopyrine, novalgin, metamizole), the sodium salt of 1-phenyl-2,3-dimethyl-4-methylaminomethanesulfonate-5-pyrazolone, is a therapeutic agent widely used as antipyretic, analgesic and antispasmodic.<sup>19,20</sup>

Flow injection techniques employing turbidimetric,<sup>21</sup> potentiometric,<sup>22</sup> amperometric,<sup>23-25</sup> spectrophotometric<sup>26-31</sup> and chemiluminescence<sup>32</sup> detections have also been successfully applied for dipyrone analysis in pharmaceuticals. In a previous work,<sup>31</sup> our group reported the method based on the generation of a blue chromophore yielded in the reaction between dipyrone and Fe(III) employing flow injection analyses. However, the present manuscript aims

to focus on a LTCC device with the optical length and the fluidic platform in the same substratum and the LED mini-photometer that was employed with the detector for a simple and fast procedure for dipyrone determination. On the other hand, there are very few published works using analytical microsystem to determine drugs in pharmaceutical formulations and there is not any work about pharmaceutical product determinations employing analytical microsystem constructed using green tapes such as LTCC coupled to a lab-made LED mini-photometer for this determination.

## Experimental

### Reagents and solutions

All solutions were prepared using Millipore (Bedford, MA, USA) Milli-Q deionized water. All chemicals were of analytical grade and used without further purification. A  $5.0 \times 10^{-3} \text{ mol L}^{-1}$  dipyrone stock solution was prepared daily by dissolving 175.7 mg of dipyrone (Aldrich) in deionized water. Reference solutions ranging from  $1.0 \times 10^{-4}$  to  $3.5 \times 10^{-3} \text{ mol L}^{-1}$  were prepared by appropriated dilutions in  $1.0 \times 10^{-2} \text{ mol L}^{-1} \text{ HNO}_3$ . A  $1.0 \times 10^{-2} \text{ mol L}^{-1} \text{ Fe}(\text{NO}_3)_3 \cdot 9\text{H}_2\text{O}$  solution was prepared by dissolving 404 mg of this salt in  $1.0 \times 10^{-2} \text{ mol L}^{-1} \text{ HNO}_3$  solution and the volume was brought up to 100 mL in a calibrated flask using the same acid solution in order to prevent hydrolysis of the Fe(III) ions.

The determination of dipyrone in commercial tablets and solutions was performed using the proposed flow injection procedure. For analysis of tablets of 500 mg, 10 tablets of the drug were used. The tablets of each formulation were weighted and powdered with a mortar and pestle. The resulting powder was diluted in  $1.0 \times 10^{-2} \text{ mol L}^{-1} \text{ HNO}_3$  solution and filtered. Suitable dilutions were made to obtain a final concentration of dipyrone within the linear range of the calibration curve.

For analyses of the solutions ( $500 \text{ mg mL}^{-1}$ ), two samples were prepared by appropriate dilutions. Subsequently, the required volume was also sampled and diluted in  $1.0 \times 10^{-2} \text{ mol L}^{-1} \text{ HNO}_3$  solution to obtain a final concentration of dipyrone within the calibration curve.

### Apparatus

A 12-channel Ismatec peristaltic pump (IPC-12) (Zurich, Switzerland) connected with Tygon<sup>®</sup> pump tubing was employed to propel the carrier and solutions.

Sample and reference solutions were inserted in the flow system with the aid of a three-piece manual injector-commutator made from Perspex containing two fixed bars and a sliding central bar.<sup>33</sup>

The radiation emitted by the LED was measured with a multi-channel USB-2000 fiber-optic spectrophotometer (Ocean Optics) coupled to an optical fiber FMD 34363 (Ocean Optics, Florida, USA).

Measurements of the molecular absorption spectrum for the blue chromophore were performed using a spectrophotometer, with linear diode array Multispec 1501 (Shimadzu, Japan), using a quartz cuvette of 1.0 cm optical path.

A lab-made LED mini-photometer was built by using an ultrabright LED AlInGaP (Agilent Technologies, model HLMP-ED-25-TW000) as a radiation source emitting light at the wavelength of maximum intensity ( $\lambda_{\max}$ ) at 630 nm, with a bandwidth ( $\lambda_{1/2\max}$ ) of 17 nm and a Si photodiode (Hamamatsu, Japan, model S1227 BR) as the photodetector. More details of the technical specifications of the LED and photodiode can be found in the manufacturer datasheet.<sup>34,35</sup> Furthermore, a digital multimeter GoldStar model DM 341 was used as analog-to-digital converter and to display the data in potential (V) on the LCD screen. A National Instruments USB interface model NI USB-6008, with a resolution of 12 bits, coupled to a microcomputer was used when necessary, as an alternative to digital multimeter, mainly for studies of time response and fast data acquisition of the LED mini-photometer.

The LED, photodiode and the microsystem constructed with LTCC technology were fixed to an acrylic support and maintained isolated from the surrounding light by using a small black box (8.0 × 6.0 × 5.0 cm) especially designed for this purpose.

A glass window (Corning 7740 (Pyrex), 1 mm thick) was used to build the optical cells, permitting a light transmission higher than 90% for wavelengths between 400 nm and 2  $\mu\text{m}$ , so it was appropriate for the used wavelength of 630 nm of this study.

For the fabrication of the microsystem, Dupont 951 (Research Triangle, USA) green ceramic tapes with 254  $\mu\text{m}$  thickness were employed. A laser (Protolaser, LPKF, Germany) and a CNC (computer numerically controlled) machine (ProtoMat, LPKF, Germany) were used for green tape machining. For the lamination and alignment of the layers, a thermo-compression press (Francisco Camps, Granollers, Spain) and programmable box furnace (Carbolite, Afora, Spain) were used, respectively.

Construction of the lab-made mini-photometer based on LED and photodiode

In Figure 1, the electronic circuit of the lab-made LED mini-photometer with the LED polarization circuit and conditioning of the signal from the Si photodiode and its connections to the digital multimeter employed as analog-to-digital converter and digital display is presented.

As shown in Figure 1, the LED was coupled to a transistor that intended to provide greater emitted radiation intensity. The maximum electric current that passed through was 58.0 mA. This electric current is within the range specified by the manufacturer datasheet. Thus, the lab-made LED mini-photometer may be used in several applications. For this specific application and in order to avoid overheating as well

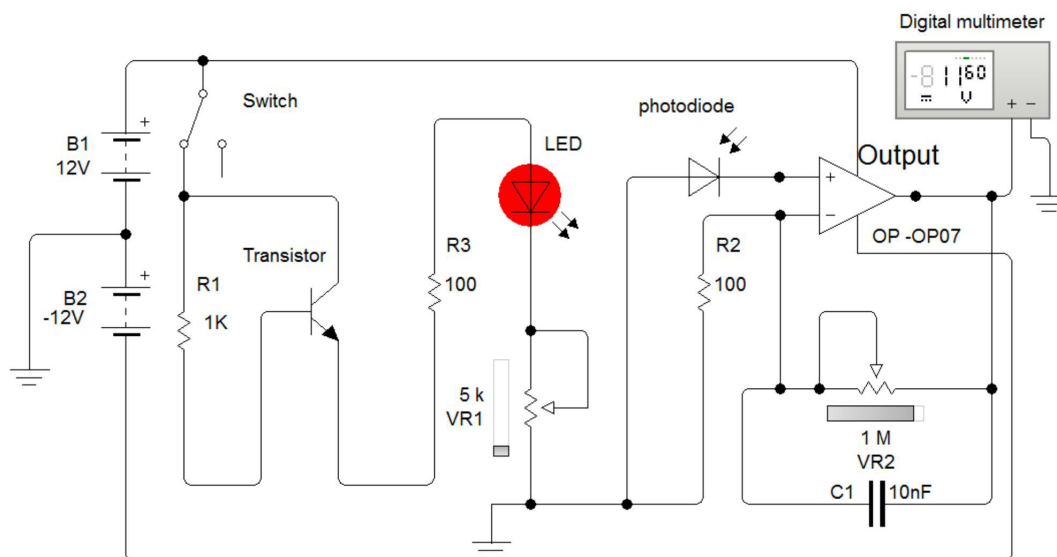


**Figure 1.** The LED polarization circuit and electronic circuit of the conditioning of the Si photodiode used in this work are presented. R1 = 1 k $\Omega$ , R2 and R3 are resistors of 100  $\Omega$ , respectively. VR1 and VR2 are variable resistors of 5 k $\Omega$  and 1 M $\Omega$ , respectively. Transistors = BC548B, B1 and B2, are two power supplies of 12 V. Red LED = AlInGaP with  $\lambda_{\max}$  = 630 nm; photodiode = S1227 (Si photodiode); OP = operational amplifier (OP07); Output = Pin 6; C1 = ceramic capacitor of 10 nF; Switch = on/off key of the mini-photometer, and digital multimeter as a display and for potential (V) measurement. A VR3 (not shown) of 5 k $\Omega$  was employed to reset the offset of the OP as presented in the Supplementary Information (SI) section, Figure S1.

as to improve the repeatability, precision, accuracy and to avoid the saturation of the sensor, the resistor R3 and variable resistor VR1 were used to control the electric current flowing to the LED, so only 2.0 mA were allowed to pass through. In order to avoid the saturation of the photosensor, the work potential was always lower than 11.60 V.

The Si photodiode was selected because of its high sensitivity at the employed wavelength (630 nm) for photometric measurements, according to the manufacturer datasheet. Because the output signal is too low, the operational amplifier OP07 was used. Using this integrated circuit, the analytical signal was amplified for more than 2800 times (2821 times).

The OP07 is very stable, presents low drift ( $1.3 \mu\text{V } ^\circ\text{C}^{-1}$ ) and low noise ( $0.6 \mu\text{V}$ ). Because the electronic circuit is very compact and employs few electronic components ( $4.0 \text{ cm} \times 4.0 \text{ cm}$ ), it was housed on either side of a black box measuring  $8.0 \text{ cm} \times 6.0 \text{ cm} \times 5.0 \text{ cm}$ .

The optical part (LED and photodiode) and analytical microsystem were fixed within the acrylic block and housed in the same box with a wall of acrylic, separating the microfluidic system from the electronic circuit to reduce the risks of accidents and short-circuiting. This black box protects the detector from external radiation which produces spurious signal.

A full description about the construction of the LED mini-photometer was incorporated in the manuscript in the Supplementary Information (SI) section (Figure S1), such as: artwork (A), arrangement of components on the printed circuit board (B), layout of the circuit (C) and a prototype of the LED mini-photometer board (D).

#### Construction of the analytical microsystem using LTCC technology

The general LTCC fabrication process for a miniaturized device was described in detail elsewhere.<sup>36-40</sup> The LTCC microsystem was constructed using green ceramic tapes individually mechanized with a laser machine and designed using the AutoCAD (Autodesk) program employing the multilayer technique. Figure 2 shows each of the layers used to construct the microsystem.

Layer A is the top and layer E is the bottom of the device. The number of layers that can compose an analytical microsystem using LTCC is variable. Generally between six and twelve layers are used.

Seven sheets of green tape were used to construct the analytical microsystem, one green tape each for layers A, B, D and E and three for layer C. The microfluidic channel in layer C was constructed with a serpentine configuration to enlarge the reactor length, allowing an enhanced mixing

Cavities to couple the brass tubes

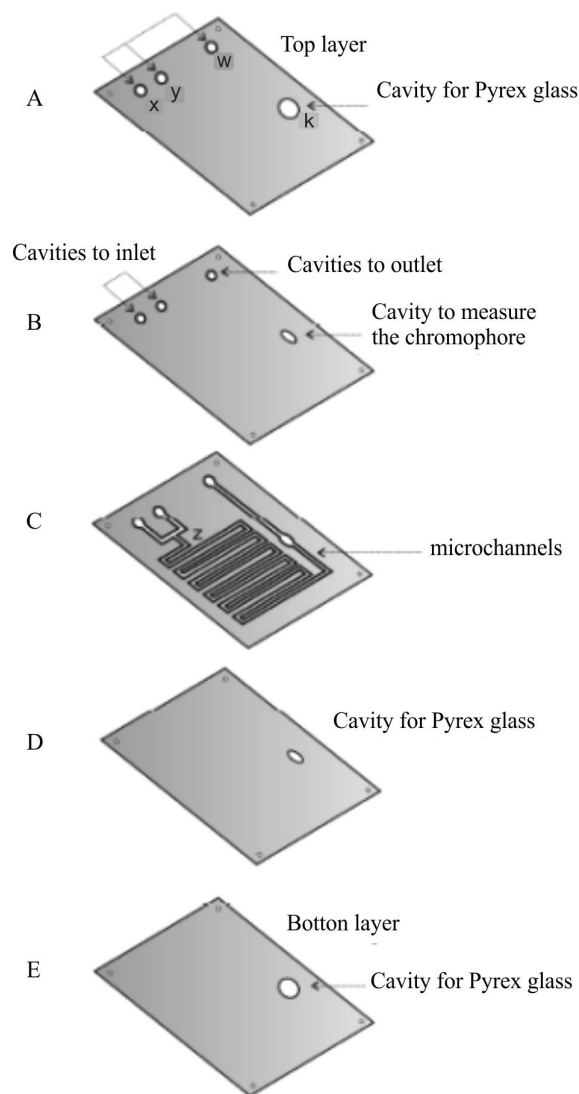


**Figure 2.** Design of the layers for construction of the analytical microsystem.

process between the reagents and the analyte and to increase residence time. Layer A defines the inlets (x and y), optical path (k) and outlet (w) of the solutions. In this layer, metallic connectors (fixed with epoxy resin) are coupled to allow the solutions to enter and exit the microsystem. The four holes in each corner of layer are used to align them during the lamination process.

Lamination of the layers to construct a single block was performed using a hydraulic press. A pressure of ca. 3000 psi was applied at  $100 \text{ }^\circ\text{C}$  for 1 min. A CNC machine was used to cut the laminated blocks to separate the different micro-devices. After that, sintering was carried out using a programmed furnace. The temperature program was selected and implemented according to the green tape manufacturer datasheet with the final temperature of  $850 \text{ }^\circ\text{C}$ .

An important point is that the design of the ceramic tapes was done taking into account that their final overlap should result in the desired three-dimensional geometry and taking into consideration that the ceramic layer will suffer ca. 15% shrinkage after the sintering process. Because of this fact, all dimensions were incremented 15% in the CAD design. In this way, the green tapes were processed to obtain micro-channels after firing 0.85 mm wide and 0.20 mm height.

After the whole process to construct the microsystem, the volumes obtained for the final reactor and optical flow cell were 55.12 and 26.68  $\mu\text{L}$ , respectively. Therefore, the total internal volume of the microsystem is 81.80  $\mu\text{L}$  and the optical path length is 0.5 mm.

#### Manifold of the flow analytical microsystem

Figure 3 shows the manifold of the flow analytical microsystem employed in this work. According to Figure 3, the reagent ( $L_1$ , 200  $\mu\text{L}$ ) and the sample or reference solution ( $L_2$ , 200  $\mu\text{L}$ ) were pumped to fill the reagent and sample loops and the excess of these solutions were propelled back to each vessel (sample vessel (SV) and reagent vessel (RV)) by a merging zone approach in order to save reagent and to reduce waste generation. Switching the injector-commutator to injection position, the selected volumes of reagent and sample (or reference solution) were simultaneously injected as individual zones in the carrier solution ( $1.0 \times 10^{-2} \text{ mol L}^{-1}$  nitric acid;  $6.0 \text{ mL min}^{-1}$ ).

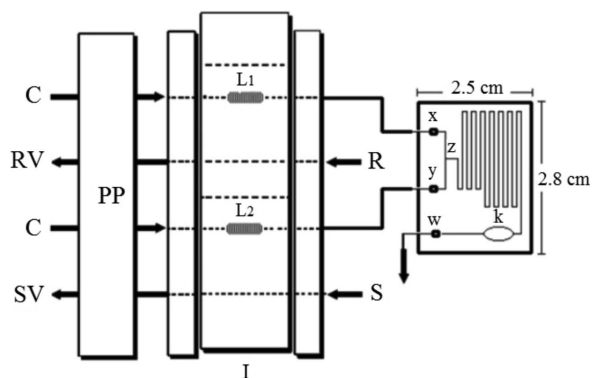


**Figure 3.** Schematic diagram of the flow injection analysis system for photometric determination of dipyrone employing an analytical microsystem constructed with LTCC technology. C = carrier solution, PP = peristaltic pump,  $L_1$  and  $L_2$  = reagent and sample looping, respectively, R and S = introduction of reagent and solution, x and y = inlet, z = confluence point, k = optical path (0.5 mm), W = outlet to waste, I = manual injector-commutator, SV = sample vessel and RV = reagent vessel.

The sample and reagent zones run for equal distances to the analytical microsystem, where the analyte enters via inlet x and the reagent via inlet y merges at a point z.

At this point, the reaction between the Fe(III) ions and dipyrone occurs generating a blue chromophore that was monitored in the optical path k (0.5 mm) employing the LED mini-photometer with measurement at 630 nm. After maximum signal measurement, the injector commutator was switched back to the initial position starting another cycle. The analytical signal caused by the chromophore generation between Fe(III) ions and dipyrone was proportional to the concentration of dipyrone in the injected solution.

#### Reference method

For accurate assessment of the results obtained by the developed procedure, the pharmaceutical formulations containing dipyrone were analyzed by iodometric titration according to the reference method.<sup>41</sup> A given amount of the pharmaceutical preparation was transferred into an Erlenmeyer flask and titrated with  $5.0 \times 10^{-2} \text{ mol L}^{-1}$  iodine solution in acetic acid, using blue iodine starch complex as an indicator.

## Results and Discussion

Performance tests, time response and data acquisition procedure of the LED mini-photometer used as photometric sensor

In order to evaluate the performance of the photometric detector, tests of rise time and stability were carried out. For this, the signal of potential (V) was estimated by the incident radiation emitted by the LED on the photodetector. This signal was suitably amplified and filtered by the operational amplifier and displayed on the LCD screen of the digital multimeter. To measure the noise level (spurious signal), the LED was switched off and a spurious signal of 4 mV was acquired. Thus, the photometric detector presented enough sensitivity to detect variation of light intensity that caused a variation of the output signal higher than 4 mV. However, when the LED was switched on, the average signal obtained was 11.285 V. Thus, an useful signal of 99.97% is available.

In order to evaluate the time response of the LED mini-photometer, a microcomputer coupled with a USB interface was used to control and receive the data. For this, a software written in Labview 8.5 was developed.

The interface consisted of 12 analog input ports and 8 digital input/output ports with a resolution of 12 bits. The AIO (analog input, pin 0) of the interface was selected for this study. According to the manufacturer datasheet, the LED and Si photodetector have a high rise time of 5.0 ns

and 5.0  $\mu\text{s}$ , respectively. However, it was just after 5 ms that the LED mini-photometer displayed the signal on the screen of the microcomputer or on the LCD screen of the multimeter. After 60 ms, the signal was quite stable with an average of 11.285 V.

The stability of the signal was monitored for 24 h, consisting of 8 h of uninterrupted monitoring on 3 different days, and a potential of  $11.285 \pm 0.003$  V with a relative standard deviation of 0.029% ( $n = 50$ ) was obtained. During these measurements, the temperature varied from 20.0 to 30.0  $^{\circ}\text{C}$ .

The good performance of the lab-made LED mini-photometer is very important to obtain satisfactory results using the developed analytical method. With this portable and inexpensive lab-made mini-photometer, the use of a microcomputer for the measurement procedure was not necessary, but it is surely possible.

To convert the measurement of potential (V) to absorbance (A) the following equation was applied:  $A = -\log(S_s/S_r) = -\log(\text{signal reading of the samples, standard solutions or blank/signal reading of reference (deionized water)})$ . It should be noted that before starting the analysis procedure, the spurious signal should be measured and subtracted from  $S_s$  and  $S_r$  in order to obtain more representative results.

#### Reaction conditions and flow injection parameters

The merging zone<sup>42,43</sup> configuration was chosen because very small volumes of reagent (Fe(III)) and sample are consumed in each injection, and provide good repeatability and high baseline stability. Initially, a UV-Vis absorption spectrum of the generated product in the reaction of dipyrone with Fe(III) ions was measured, as shown in Figure 4.

In this experiment, a  $1.0 \times 10^{-3}$  mol L<sup>-1</sup> dipyrone solution,  $1.0 \times 10^{-2}$  mol L<sup>-1</sup> iron(III) nitrate in  $1.0 \times 10^{-2}$  mol L<sup>-1</sup> nitric acid solution and a quartz cuvette of 1.0 cm optical path were employed. The maximum analytical signal was reached in the wavelength of 622 nm, hence, the LED with  $\lambda_{\text{max}}$  at  $630 \pm 17$  nm was selected for this study.

The formation of the chromophore was observed beginning at the first second of the reaction between dipyrone and the Fe(III) ions. Additionally, as can be seen from the axis of the time of the above mentioned figure, the chromophore formed was relatively unstable, with a lifetime of 40 s in these experimental conditions.

The instability of this complex seems to be caused by photoreduction process.<sup>44</sup> However, by employing the flow injection system developed in this work, it was possible to monitor unstable compounds. Thus, the chromophore concentration was detected without loss of sensitivity (inclination of analytical curve), with good accuracy and precision.

For this purpose, it was necessary to adjust some of the parameters in the configuration of the flow system, such as reduction of the helicoidal loop length and/or increase of the flow rate of the carrier solution. Several parameters were optimized in order to achieve the optimal conditions to promote the reaction between dipyrone and Fe(III) ions, in an acid medium.

Chemical and flow injection parameters were optimized by using the univariate method in order to reach the best analytical signal, sample throughput, repeatability and stability of the baseline. These studies were carried out using a standard solution containing  $5.0 \times 10^{-4}$  mol L<sup>-1</sup> of dipyrone.

The effect of HNO<sub>3</sub> concentration used as the carrier was investigated in the concentration range from  $1.0 \times 10^{-3}$  to 0.1 mol L<sup>-1</sup>. The analytical signal increased with

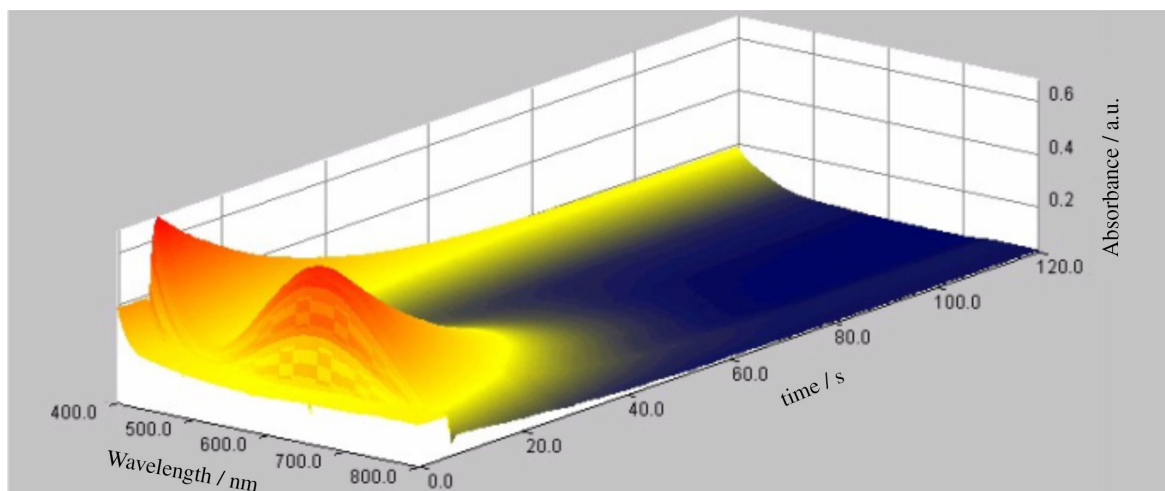


**Figure 4.** 3D absorption spectrum of blue chromophore ( $\lambda_{\text{max}} = 630$  nm).

the  $\text{HNO}_3$  concentration up to  $1.0 \times 10^{-2} \text{ mol L}^{-1}$  and remained constant in higher concentrations. Therefore, a  $1.0 \times 10^{-2} \text{ mol L}^{-1}$   $\text{HNO}_3$  solution was selected in all further experiments.

The influence of the Fe(III) ion concentrations on the analytical signal in the concentration range from  $1.0 \times 10^{-3}$  to  $3.0 \times 10^{-2} \text{ mol L}^{-1}$  were studied. It was observed that the signal increased with the Fe(III) concentration up to  $1.0 \times 10^{-2} \text{ mol L}^{-1}$ , and remained practically constant up to a concentration of  $3.0 \times 10^{-2} \text{ mol L}^{-1}$ . Thus, a  $1.0 \times 10^{-2} \text{ mol L}^{-1}$  Fe(III) solution was chosen for further experiments to save reagent and to decrease waste generation.

The effect of the injected sample and reagent volumes was evaluated by simultaneous variation of the  $L_1$  and  $L_2$  loop volumes between 100-500  $\mu\text{L}$ . The analytical signal increased with greater volumes up to 200  $\mu\text{L}$  for the sample and reagent, above which the analytical signal remained practically constant. Sample and reagent volumes of 200  $\mu\text{L}$  were chosen as a good compromise between analytical signal, repeatability, sample throughput and waste generation.

The flow rate was investigated in the range of 1.2 to 11.0  $\text{mL min}^{-1}$ . It was found that the best analytical signals were reached using a carrier flow rate of 5.0  $\text{mL min}^{-1}$ , however in flow rates of approximately 6.0  $\text{mL min}^{-1}$  the analytical signal remained practically constant. However, the flow rate of 6.0  $\text{mL min}^{-1}$  was chosen because it reached a higher sample throughput. Thus, this flow rate was established for further experiments.

#### Recovery test and potential interference

Recoveries of 98.0-103.6% dipyrone from six pharmaceutical formulations were obtained using the flow injection analysis (FIA) procedure. In this study,  $2.0 \times 10^{-4}$ ,  $4.0 \times 10^{-4}$  and  $5.0 \times 10^{-4} \text{ mol L}^{-1}$  of dipyrone were added to each pharmaceutical product. The obtained recovery results suggested an absence of the matrix effect in the determination of dipyrone in these samples. Using the flow injection setup shown in Figure 3, under optimal conditions previously described, the interference effect of several common pharmaceutical excipients on the determination of dipyrone was examined.

The selectivity of the flow injection procedure was investigated using solutions containing  $5.0 \times 10^{-4} \text{ mol L}^{-1}$  of dipyrone added to various concentrations of potential interferents. Caffeine, sodium monophosphate, sorbitol, sodium chloride, saccharin, glycerin, sucrose and fructose did not interfere even when present in concentrations much higher than those commonly found in pharmaceutical

products. The reagent consumption was 0.8 mg of  $\text{Fe}(\text{NO}_3)_3 \cdot 9\text{H}_2\text{O}$  per determination.

#### Analytical features and applications

The calibration graph for the dipyrone determination was linear in the range of  $1.0 \times 10^{-4}$  to  $3.5 \times 10^{-3} \text{ mol L}^{-1}$  ( $A = 0.00907 + 91.70 [C]$ ;  $r = 0.999$ , where  $A$  is the absorbance and  $[C]$  the concentration of dipyrone in  $\text{mol L}^{-1}$ ). A limit of detection of  $4.5 \times 10^{-5} \text{ mol L}^{-1}$  (three times the blank relative standard deviation/slope of the analytical curve) and relative standard deviation (RSD) less than 0.5% ( $n = 10$ ) for  $5.0 \times 10^{-4}$  and  $2.0 \times 10^{-3} \text{ mol L}^{-1}$  of dipyrone solutions were obtained. An analytical frequency of 195  $\text{h}^{-1}$  was achieved, indicating a fast back to baseline signal without carry-over problems, which indicated the non-existence of reagent accumulation within the analytical microsystem. Typical transient signals are shown in Figure 5.

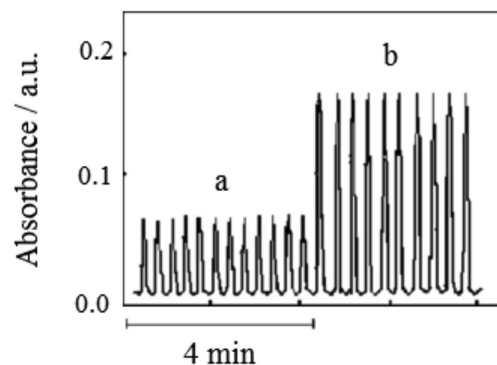


**Figure 5.** Repeatability study, conditions: injection volume of 200  $\mu\text{L}$ , dipyrone concentration of (a)  $5.0 \times 10^{-4}$  and (b)  $2.0 \times 10^{-3} \text{ mol L}^{-1}$ , flow rate of 6.0  $\text{mL min}^{-1}$ .

Results of the analysis are presented in Table 1. As it can be seen, good agreements between the results obtained in the determination of dipyrone by the developed FIA procedure and the titrimetric method described in the Brazilian Pharmacopoeia<sup>39</sup> were found by using the  $t$ -test (2, 2, 95%), confirming the accuracy of the flow injection photometric method. The proposed method showed a higher sample throughput than the existing flow injection procedures.<sup>21-31</sup> Even with the reduced optical path, the developed procedure showed better limits of detection than the previous published works<sup>21,22,27,31</sup> dedicated to the determination of dipyrone. Additionally, by comparing the figures of merit of the proposed procedure and the ones previously published,<sup>31</sup> in which the same reaction was performed, a lower waste generation (480  $\mu\text{L}$  vs. 1000  $\mu\text{L}$ ) and a higher analytical throughput (195  $\text{h}^{-1}$  vs. 80  $\text{h}^{-1}$ ) were acquired in the present work. In

**Table 1.** Determination of dipyrone in pharmaceutical formulations using the reference method and the proposed flow injection procedure

Sample	Labeled	Dipyrone		Relative error / %	
		Reference method	Developed procedure	E <sub>R1</sub>	E <sub>R2</sub>
A	500.0 <sup>a</sup>	503.2 ± 0.6	520.2 ± 0.4	4.0	3.4
B	500.0 <sup>a</sup>	489.2 ± 0.4	481.1 ± 0.3	-3.8	-1.7
C	500.0 <sup>a</sup>	494.6 ± 0.4	501.5 ± 0.4	0.3	1.4
D	500.0 <sup>a</sup>	509.1 ± 0.3	504.6 ± 0.3	0.9	-0.9
E	500.0 <sup>b</sup>	504.3 ± 0.4	510.2 ± 0.7	2.0	1.2
F	500.0 <sup>b</sup>	510.5 ± 0.1	514.2 ± 0.4	2.8	0.7

<sup>a</sup>mg tablet<sup>-1</sup>; <sup>b</sup>mg mL<sup>-1</sup>; *n* = 3, mean ± standard deviation, confidence level 95%. E<sub>R1</sub>: relative error for flow procedure vs. labeled value; E<sub>R2</sub>: relative error for flow procedure vs. reference method.

fact, these features were reached due to the use of a LTCC as cuvette, mixer and low volume chamber. However, the limit of detection (LOD) obtained in the present work was 20 times higher ( $4.5 \times 10^{-5}$  mol L<sup>-1</sup> (proposed) vs.  $2.3 \times 10^{-6}$  mol L<sup>-1</sup>). This reduction in LOD was expected since the optical path of the LTCC (0.5 mm) was 20 times smaller (1.0 cm, conventional for commercial cuvette). But this does not compromise the performance of the proposed analytical procedure since the concentration of analytes in pharmaceutical formulations such as dipyrone is generally high. Besides, the discrepancy in the LOD values was due to the different optical paths, thus, the use of a LED mini-photometer as detector replaces the commercial spectrophotometer satisfactorily with good performance, which is another advantage of the present work. Moreover, a simple multimeter can be used to acquire the results of the LED mini-photometer during the analytical procedure, as well as the USB interface coupled to a microcomputer, if necessary.

## Conclusions

The analytical microsystem based on LTCC technology described in this work showed to be a useful tool for dipyrone determination in pharmaceuticals, and can also be extended to the determination of other drugs. This work showed the ease of constructing miniaturized analytical systems using low-temperature co-fired ceramic technology and a lab-made LED mini-photometer as photodetector.

Despite its simplicity and the use of low-cost electronic components, the performance of the developed photodetector was not compromised, as seen in the obtained results: satisfactory stability, low drift and good sensitivity. In fact, the results obtained for the determination of dipyrone in commercial formulations using the flow analytical microsystems based on LTCC and a lab-made

LED mini-photometer were in good agreement with those obtained by the reference method when compared using a *t*-paired test at a confidence level of 95%.

The developed method is fast (higher sample throughput), sufficiently sensitive, accurate and precise. These features make it suitable for routine analysis and quality control of pharmaceutical samples in laboratories. Moreover, there are very few published data using analytical microsystem to determine drugs in pharmaceutical formulations and there is not any work about pharmaceutical product determination employing analytical microsystems constructed using green tapes coupled to a lab-made mini-photometer, leading to a compact, robust, environmentally friendly and efficient analytical flow system for dipyrone determination in commercial formulations.

## Supplementary Information

Supplementary information on the development of the LED mini-photometer (Figure S1) is available free of charge at <http://jbcs.sbq.org.br> as a PDF file.

## Acknowledgments

The authors are grateful to the Fundação de Amparo à Pesquisa do Estado de Minas Gerais (Fapemig), the Conselho Nacional de Desenvolvimento Científico e Tecnológico (CNPq) and to the Coordenação de Aperfeiçoamento de Pessoal de Nível Superior (CAPES).

## Reference

1. Dittrich, P. S.; Tachikawa K.; Manz, A.; *Anal. Chem.* **2006**, *78*, 3887.
2. Vilkner, T.; Janasek, D.; Manz, A.; *Anal. Chem.* **2004**, *76*, 3373.
3. Reyes, D. R.; Iossifidis, D.; Aurox, P. A.; Manz, A.; *Anal. Chem.* **2002**, *74*, 2623.



4. Ibáñez-García, N.; Martínez-Cisneros, C. S.; Valdés, F.; Alonso, J.; *TrAC, Trends Anal. Chem.* **2008**, *27*, 24.
5. Gongora-Rubio, M. R.; Espinoza-Vallejos, P.; Sola-Laguna, L.; Santiago-Avilés, J. J.; *Sens. Actuators, A* **2001**, *89*, 222.
6. Achmann, S.; Hammerle, M.; Kita, J.; Moos, R.; *Sens. Actuators, B* **2008**, *135*, 89.
7. Bemnowicz, P.; Golonka, L. J.; *J. Eur. Ceram. Soc.* **2010**, *30*, 743.
8. Coltro, W. K. T.; Piccin, E.; Carrilho, E.; de Jesus, D. P.; da Silva, J. A. F.; da Silva, H. D. T.; Lago, C. L.; *Quim. Nova* **2007**, *30*, 1986.
9. Ródenas-Torralba, E.; Rocha, F. R. P.; Reis, B. F.; Morales-Rubio, A.; de la Guardia, M.; *J. Autom. Methods Manage. Chem.* **2006**, *2006*, 1.
10. Palma, A. J.; Ortigosa, J. M.; Lapresta-Fernandez, A.; Fernandez-Ramos, M. D.; Carvajal, M. A.; Capitan-Vallvey, L. F.; *Rev. Sci. Instrum.* **2008**, *79*, 103.
11. Pires, C. K.; Reis, B. F.; Morales-Rubio, A.; de la Guardia, M.; *Talanta*, **2007**, *72*, 1370.
12. Tzanavaras, P. D.; Themelis, D. G.; *Anal. Chim. Acta* **2007**, *588*, 1.
13. Ruzicka, J.; Hansen, E. H.; *TrAC, Trends Anal. Chem.* **2008**, *27*, 390.
14. Ruzicka J.; Hansen, E. H.; *Anal. Chem.* **2000**, *72*, 212.
15. Grabowska, I.; Ksok, E.; Wyzkiewicz, I.; Chudy, M.; *Microchim. Acta* **2009**, *164*, 299.
16. Wang, J.; Pumera, M.; *Talanta* **2006**, *69*, 984.
17. Baeza, M. D. M.; Ibáñez-García, N.; Baucells, J.; Bartroli, J.; Alonso, J.; *Analyst* **2006**, *131*, 1109.
18. Zhang, Z. J.; He, D. Y.; Liu, W.; Lv, Y.; *Luminescence* **2005**, *20*, 377.
19. Gulmez, S. E.; Serel, S.; Uluc, A.; Can, Z.; Ergun, H.; *Aesth. Plast. Surg.* **2008**, *32*, 766.
20. Levy, M.; Zylberkat, E.; Rosenkranz, B.; *Clin. Pharmacokinet.* **1995**, *28*, 216.
21. Marcolino-Junior, L. H.; Bonifácio, V. G.; Fatibello-Filho, O.; Teixeira, M. F. S.; *Quim. Nova* **2005**, *28*, 783.
22. Albuquerque, J. S.; Silva, V. L.; Lima, F.; Araújo, A. N.; Montenegro, M. C. B. S. M.; *Anal. Sci.* **2003**, *19*, 691.
23. Muñoz, R. A. A.; Matos, R. C.; Angnes, L.; *J. Pharm. Sci.* **2001**, *90*, 1972.
24. Perez-Ruiz, T.; Lozano, C. M.; Tomas, V.; *J. Pharm. Biomed. Anal.* **1994**, *12*, 1109.
25. Boni, A. C.; Wong, A.; Dutra, R. A. F.; Sotomayor, M. D. T.; *Talanta* **2011**, *85*, 2067.
26. Lima, J. L. F. C.; Sá, S. M. O.; Santos, J. L. M.; Zagatto, E. A. G.; *J. Pharm. Biomed. Anal.* **2003**, *32*, 1011.
27. Marcolino-Júnior, L. H.; Sousa, R. A.; Fatibello-Filho, O.; Moraes, F. C.; Teixeira, M. F. S.; *Anal. Lett.* **2005**, *38*, 2315.
28. Weinert, P. L.; Fernandes, J. R.; Pezza, L.; Pezza, H. R.; *Anal. Sci.* **2007**, *23*, 1383.
29. Krug, F. J.; Bergamin, H.; Zagatto, E. A. G.; *Anal. Chim. Acta* **1986**, *179*, 103.
30. Schmidt, E.; Melchert, W. R.; Rocha, F. R. P.; *Quim. Nova* **2011**, *34*, 1205.
31. Suarez, W. T.; Pessoa-Neto, O.; Vicentini, F. C.; Janegitz, B. C.; Faria, R. C.; Fatibello-Filho, O.; *Anal. Lett.* **2011**, *44*, 340.
32. Peres, J. A. P.; Alegria, J. S. D.; Hernando, P. F.; Sierra, A. N.; *Luminescence* **2012**, *27*, 45.
33. Bergamin, H.; Zagatto, E. A. G.; Krug, F. J.; Reis, B. F.; *Anal. Chim. Acta* **1978**, *101*, 17.
34. <http://www.digchip.com/datasheets/parts/datasheet/021/HLMP-ED25-TW000-pdf.php> accessed in February 2013.
35. [http://sales.hamamatsu.com/assets/pdf/parts\\_S/S1227\\_series.pdf](http://sales.hamamatsu.com/assets/pdf/parts_S/S1227_series.pdf) accessed in July 2012.
36. Ibáñez-García, N.; Puyol, M.; Azevedo, C. M.; Martínez-Cisneros, C. S.; Villuendas, F.; Gongora-Rubio, M. R.; Seabra, A. C.; Alonso, J.; *Anal. Chem.* **2008**, *80*, 5320.
37. Llopis, X.; Ibáñez-García, N.; Alegret, S.; Alonso, J.; *Anal. Chem.* **2007**, *79*, 3662.
38. Ibáñez-García, N.; Mercader, M. B.; da Rocha, Z. M.; Seabra, A. C.; Gongora-Rubio, M. R.; Chamarro, J. A.; *Anal. Chem.* **2006**, *78*, 2985.
39. Ibáñez-García, N.; Goncalves, R. D. M.; da Rocha, Z. M.; Gongora-Rubio, M. R.; Seabra, A. C.; Chamarro, J. A.; *Sens. Actuators, B* **2006**, *118*, 67.
40. Alves-Segundo, R.; Ibáñez-García, N.; Baeza, M.; Puyol, M.; Alonso-Chamarro, J.; *Microchim. Acta* **2011**, *172*, 225.
41. *Brazilian Pharmacopoeia*, 3<sup>rd</sup> ed.; Andrei Editora S.A.; São Paulo, Brazil, 1977, p. 71.
42. Canaes, L. S.; Leite, O. D.; Fatibello-Filho, O.; *Talanta* **2006**, *69*, 239.
43. Piccin, E.; Vieira, H. J.; Fatibello-Filho, O.; *Anal. Lett.* **2005**, *38*, 511.
44. Qureshi, S. Z.; Saeed, A.; Haque, S.; *Microchem. J.* **1990**, *41*, 362.

Submitted: September 21, 2012

Published online: May 15, 2013

FAPESP has sponsored the publication of this article.